


Article

The Impact of Aging-Preventive Algorithms on BESS Sizing under AGC Performance Standards

Cristobal Morales ¹, Augusto Lismayes ¹, Hector Chavez ^{2,*} , Harold R. Chamorro ^{3,*} and Lorenzo Reyes-Chamorro ⁴

¹ Departamento de Ingenieria Electrica, Universidad de Santiago de Chile, Estación Central, Santiago 9170197, Chile; cristobal.morales@usach.cl (C.M.); augusto.lismayes@usach.cl (A.L.)

² Departamento de Ingenieria Electrica (Innovative Energy Technologies Center, INVENT UACH), Universidad de Santiago de Chile, Estación Central, Santiago 9170197, Chile

³ KTH, Royal Institute of Technology, SE-100 44 Stockholm, Sweden

⁴ Facultad de Ciencias de la Ingeniería (Innovative Energy Technologies Center, INVENT UACH), Institute of Electricity and Electronics, Universidad Austral de Chile, Valdivia 5110566, Chile; lorenzo.reyes@uach.cl

* Correspondence: hector.chavez@usach.cl (H.C.); hr.chamo@ieee.org (H.R.C.)

Abstract: It is normally accepted that Battery Energy Storage Systems improve frequency regulation by providing fast response to the Automatic Generation Control. However, currently available control strategies may lead to early Energy Storage Systems aging given that Automatic Generation Control requirements are increasing due to zero carbon power generation integration. In this sense, it is important to analyze the aging phenomena in order to assess the technical–economical usefulness of Battery Energy Storage Systems towards zero carbon power systems. In order to avoid early aging, various proposals on aging-reducing algorithms can be found; however, it is unclear if those aging-reducing algorithms affect the performance of Battery Energy Storage Systems. It is also unclear whether those effects must be internalized to properly dimension the capacity of Battery Energy Storage Systems to both comply with performance standards and to prevent early aging. Thus, this paper estimates the storage capacity of a Battery Energy Storage Systems to comply with Automatic Generation Control performance standard under aging-reducing operating algorithms by dynamics simulations of a reduced-order, empirically-validated model of the Electric Reliability Council of Texas. The results show the relationship between the required performance of Automatic Generation Control and Battery Energy Storage System capacity, considering a 1-year simulation of Automatic Generation Control dynamics. It can be concluded that the compliance with performance standards is strongly related to the storage capacity, regardless of how fast the device can inject or withdraw power from the grid. Previous results in the state-of-the-art overlook the quantification of this relationship between compliance with performance standards and storage capacity.

Keywords: Energy Storage System; Automatic Generation Control; BESS sizing



Citation: Morales, C.; Lismayes, A.; Chavez, H.; Chamorro, H.R.; Reyes-Chamorro, L. The Impact of Aging-Preventive Algorithms on BESS Sizing under AGC Performance Standards. *Energies* **2021**, *14*, 7231. <https://doi.org/10.3390/en14217231>

Academic Editor: Elyas Rakhshani

Received: 13 September 2021

Accepted: 13 October 2021

Published: 2 November 2021

Publisher's Note: MDPI stays neutral with regard to jurisdictional claims in published maps and institutional affiliations.



Copyright: © 2021 by the authors. Licensee MDPI, Basel, Switzerland. This article is an open access article distributed under the terms and conditions of the Creative Commons Attribution (CC BY) license (<https://creativecommons.org/licenses/by/4.0/>).

1. Introduction

The rapid increase of intermittent sources of generation has brought significant challenges to power system operations. The low to zero inertia of this type of generation technology, the high variability of the associated resources, and their limited frequency-responsiveness have deteriorated the capability of power systems to maintain the power balance [1].

Several types of energy storage technologies have been proposed as possible solutions in the literature [2]. One can find synchronous condensers, flywheels and high capacity storage batteries whose ramping capability per unit of installed capacity is significantly larger than that of conventional generating units providing Secondary Frequency Control (SFC). In general, Battery Energy Storage Systems (BESS) are widely accepted as a technical solution to the increasing intermittent generation integration [3].

Although BESS represents a technical solution to the increasing need for flexibility in power systems, there are various techno-economic aspects that complexify the analysis. On one hand, the life cycle of BESS are strongly affected by their operating regime [4]. While simple models account for the number of cycles to assess the life time of a BESS, more sophisticated approaches take into account environmental variables and minute-to-minute charge/discharge operation [5]. This way, aging-minimizing algorithms prevent BESS fast movements, by filtering input charge/discharge commands from the Automatic Generation Control system (AGC) in order to preserve the integrity of the BESS in the long term. These aging-preventive algorithms are very important for BESS vendors, as they preserve the lifetime within manufacturer warranties; the same applies for investors, that need a certain/fixed lifetime for the BESS to properly analyze profitability. On the other hand, SFC BESS business models (on the investor side) depend on the payments from Ancillary Service Markets that also depend upon compliance with AGC performance standards in California, United States [6], the Midwest of the United States [7] and China [8]. As the aging-preventive algorithms are strongly related to State of Charge (SoC), a BESS with relatively large storage time (MWh of energy storage divided by the MW of power deliverability) will prevent large differences between AGC power commands and BESS power output. However, a larger storage time leads to a larger cost, which negatively affects the economic feasibility of the BESS. In this sense, the common idea of BESS being the solution to carbon neutral energy integration must be contrasted with the costs of that solution to be a feasible alternative. In terms of costs, BESS size comprises a high share of the total costs and it must be analyzed. The relationship between BESS size and AGC performance has not captured particular attention in the literature.

State of the Art

Most sizing algorithms for BESS normally overlook the impact of the AGC performance standard under aging-preventive algorithms. The main aspect that BESS sizing algorithms consider is the trade-off between the technical improvements and the costs of those improvements with respect to the additional benefits [9]. In that sense, particular advancements can be found in terms of BESS-demand coordination [10], BESS-Supercapacitor coordination [11], and BESS-co-generation at the residential level [12]. In terms of aging estimation techniques, there are numerous works on improved aging models [13], data-driven methods [14], use of transfer component analysis to improve data-driven aging models [15], adaptive Kalman filter estimation [16], continuous time aging estimation [17], and physical parameter identification [18]. The progress on estimating BESS aging is significant, but its relation to power system frequency control operation is visited in relatively few specialized works.

In terms of BESS as SFC providers, there is also abundant literature with little focus on the impact of aging on AGC performance. The majority of the works focus on operating aspects, such as the dynamic modeling of BESS considering aging representations [19] or SoC balancing strategies under diverse BESS applications [20]. In [21], the effect of aging-preventive algorithms on AGC BESS performance is addressed by the definition of dynamic AGC signals, which basically undercover the underlying issue of not complying with the dynamic requirements by differentiating the AGC signal with technology. The effect of SoC constraints on AGC dynamics is also exposed in [22], emphasizing the importance of such constraints in the performance of AGC. However, the effect of those constraints in the sizing of BESS is not considered in detail. Ref. [23] presents an operation strategy based on economic aspects and the degradation of the BESS. Different operational policies are considered, focusing on constraining the SoC to reduce degradation. Although the work considers the impact of aging in BESS sizing, it overlooks the impacts on AGC performance that depend on the real-time operation of AGC.

This work considers an exploratory simulation to assess the effects of aging-preventive algorithms on AGC BESS performance in order to obtain the smallest BESS size that can comply with AGC performance standards from current practices. An empirically-

validated, reduced-order model of frequency dynamics is considered for the case of the Reliability Council of Texas (ERCOT), and a simple model of an aging-preventive algorithm is considered to obtain numerical results. These results answer a central question in the transition to carbon neutral power systems, regarding a proper estimation of the BESS capacity to maintaining AGC performance under the penetration of wind power.

2. Dynamic Models

This section describes the empirical dynamic model of SFC, the AGC control loop, and the BESS dynamics and operation.

2.1. AGC System

The AGC regulates the minute-to-minute frequency deviations. The model used is based on [24], consisting of a proportional gain K_{AGC} . From [24], it is assumed that the reserves and ramp capacity of the system are sufficient to follow the AGC signal. The above constraints are introduced to the model as explained in [25]. The control diagram is presented in Figure 1.

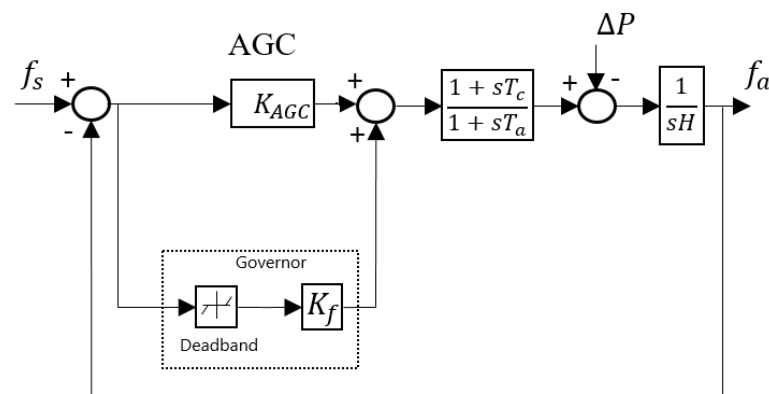


Figure 1. Frequency dynamics model.

In Figure 1, H is the inertial constant in (MWs/Hz), T_a is the governor time constant, T_c is the governor phase time constant, K_f (MW/Hz) is the governor droop, f_s is the scheduled frequency, f_a is the actual frequency, and ΔP is the power imbalance. In [25], the following expression was determined for the AGC gain.

$$K_{AGC} \geq \frac{\sigma_{NLI_{1m}}}{\epsilon}, \quad (1)$$

where $\sigma_{NLI_{1m}}$ is the standard deviation of 1-min system frequency samples obtained over a year of operation, and ϵ (Hz) is an index that represents the desired standard deviation of the 1-year histogram of frequency deviations in Hz. Normally, ϵ is given by the Electrical authority; in the case of ERCOT, $\epsilon = 30$ mHz.

In order for the model to represent an actual instance of the ERCOT system, a data-driven approach was considered. In general, the dynamics of the system is mostly driven by generation and load, among which generation has the most relevant role. In terms of frequency dynamics, the largest contribution comes from inertia and governor response that is provided by synchronous generation, while wind and solar power account for a low to zero contribution. This way, one can associate frequency dynamics with the number of synchronous machines online, that is roughly associated with system load that is not provided by solar or wind. Then, Netload N_L is a good descriptor of power system frequency dynamics.

In [26], a data analytic technique is used to find a relationship between N_L and the most relevant parameters of the model in Figure 1, namely H , T_a , T_c and K_f . From synchrophasor measurement of the ERCOT frequency under various operating conditions, the parameters

of the model in Figure 1 where identified to represent the measured behavior, and the following relationships were found between the parameters and Netload:

$$H = 397.63 + 0.23003 \cdot NL \quad (2)$$

$$T_a = 3.4673 + 1.9372 \cdot 10^{-5} \cdot NL \quad (3)$$

$$T_c = 0.64866 + 2.2526 \cdot 10^{-5} \cdot NL \quad (4)$$

$$K_f = 2138.7 + 0.12312 \cdot NL. \quad (5)$$

This way, the model can capture the dynamics of the system for various conditions that continuously change with NL in reality.

2.2. Dynamic of the BESS

In order to represent the general aspects of BESS dynamics, this work considered the model presented in [27]. There are BESS models that represent the underlying chemical and thermodynamic characteristics of BESS; however, those characteristics do not significantly contribute to the power and energy dynamics in the seconds-to-minutes time scale, in which SFC phenomena occur. The discrete time model in [27] represents the dominant dynamic aspects for the purpose of SFC analysis as follows:

$$SOC_{t+1} = SOC_t - \frac{T_{int}}{60} (P_t^{EES+}) \frac{1}{\sqrt{\eta}} + \frac{T_{int}}{60} (P_t^{EES-}) \sqrt{\eta}, \quad (6)$$

where t is the discrete time-step, SOC_t is the SoC state at time t , T_{int} (minutes) is the time step operation, η is the input-output efficiency of the BESS, P_t^{EES+} is the discharge power output at time t , and P_t^{EES-} is the charge power output at time t . The model represents the change in SoC with respect to the input and output power of the BESS, and the losses in the chemical process and the switching losses of the power electronic converter. Note that, for simplicity, SoC is measured in term of energy.

2.3. BESS Aging-Preventing Operation and Strategy for SFC

The aging process of a battery is very complex and is subject of intense research [28]. In general, various complex techniques to prevent aging have been proposed for the case of small residential storage devices [29], electric vehicles [13], and large-scale BESS for power systems [21,30]. The model in [21] has been used in various studies comprising power system analysis [22,31] for AGC applications, so it is considered as suitable for the proposed study.

The model first considers limitations respect to BESS SOC maximum value (SOC_{max}) and minimum value (SOC_{min}). To prevent out-of-limit operation, the power output P_t^{EES+} / P_t^{EES-} of the BESS is set to zero in the case that the SOC calculated by (6) is outside of the accepted range. Otherwise, the power output is set to the power required by the AGC command. This way, the SoC limits are not violated.

In terms of preventing early aging, Ref. [21] considers a filtered version of the AGC signal for the BESS. To this end, a dynamic capacity of the BESS is defined—namely Dynamic Available AGC (DAA) in MW—as the sustainable 1-min charge/discharge power the BESS can withstand with no additional aging effects. The DAA is continuously updated on a 1-min basis, so it is possible to adjust the output power of the BESS as a function of the SOC. The DAA capability definition is shown in (7).

$$DAA_t = \begin{cases} \min\left\{\frac{(E_{max} - E_t)}{T_{int}}, P_{nom}\right\} & ; AGC_t \leq 0 \\ \min\left\{\frac{(E_t - E_{min})}{T_{int}}, P_{nom}\right\} & ; AGC_t \geq 0, \end{cases} \quad (7)$$

where DAA_t and AGC_t are the Dynamic Available and AGC signal respectively in the i interval, E_t (MWh) is the energy stored by the BESS at time t , E_{max} and E_{min} are the

maximum and minimum allowable energy for the BESS, P_{nom} is the nominal power of the BESS, and T_{int} is the time step of the simulation equal to 1 min. In general, E_t is a function of the SoC of the BESS given by lookup tables [21]; for this work, E_t will be assumed proportional to SoC and the nameplate energy capacity of the BESS.

Then, there will be one AGC signal for the BESS units (namely AGC_{BESS}) and an AGC signal for the rest of the units (namely AGC_{GEN}). The AGC signal definitions are shown in (9).

$$AGC_{BESS} = AGC \frac{DAA_{BESS}}{DAA_{BESS} + DAA_{GEN}} \quad (8)$$

$$AGC_{GEN} = AGC - AGC_{BESS}, \quad (9)$$

where DAA_{GEN} and DAA_{BESS} are the total reserve from conventional generators and BESS for the SFC, respectively.

The frequency control including BESS is shown in Figure 2, where the operating strategy is presented in a simplified scheme.

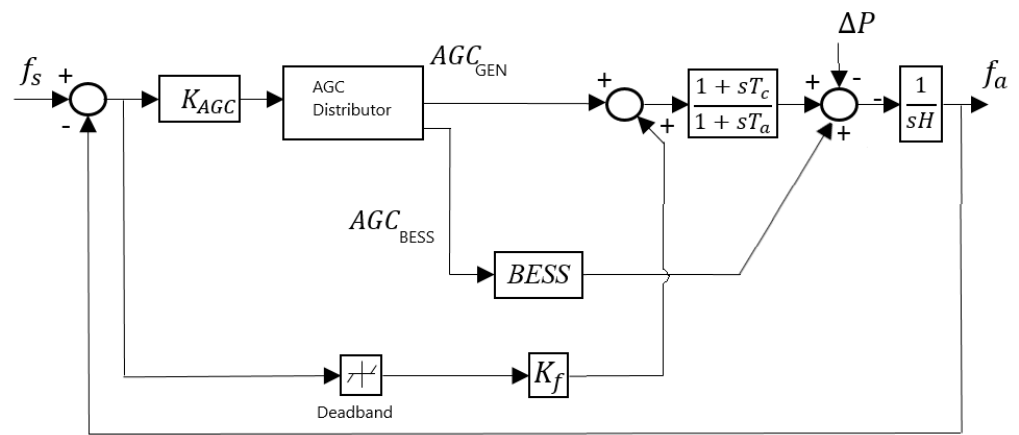


Figure 2. BESS operation strategy.

3. Criteria for BESS Capacity Estimation

As mentioned in Section 1, units providing SFC must comply with performance standards in order to qualify for ancillary service payments; however, the aging-preventive algorithms can prevent proper compliance of BESS to SFC. Considering that most of the aging-preventive algorithms take into consideration the movements of the BESS output power respect to its SoC state, a large BESS capacity will likely prevent any noncompliance. This way, there is a trade-off between increasing the BESS capacity to prevent noncompliance and the cost of the additional BESS capacity. This work will explore the minimum BESS capacity under which compliance can be obtained through simulations.

3.1. Error Indicator of AGC Tracking

As to represent SFC compliance, the indicator used in this work, expressed in (10), will be the absolute error in the tracking of the AGC, defined by the CAISO (California Independent System Operator) system in [7].

$$Noncompliance(\%) = \frac{\sum_{\tau=1}^N |P_{set}(\tau) - P_{real}(\tau)|}{\sum_{\tau=1}^T P_{set}(\tau)} \times 100\%, \quad (10)$$

where N is the number of periods for which the index is calculated, P_{set} is the required power by the AGC signal and P_{real} actual power delivered by the BESS. In (10), the indicator is expressed as a Noncompliance since it establishes the absolute energy (*mileage* [7]) not provided by the BESS. Consequently, the difference between energy required by the AGC and the energy actually delivered by the BESS is represented. In this work, it is assumed

that the ramp capacity of the BESS is sufficient to respond to the requirements of the AGC, so the operational deficit will depend on the available energy, in other words, it will depend mainly on the storage capacity.

3.2. Performance Criteria

To evaluate the performance of the BESS in the SFC, the compliance criterion expressed in (11) has been used, similar to the one used by the MISO (Midcontinent Independent System Operator) system in [8].

$$Deficit = \begin{cases} Pass; & Noncompliance \leq 30\% \\ Fail; & Noncompliance > 30\%. \end{cases} \quad (11)$$

In the context of this work, according to (11), the BESS does not satisfy the requirements of the system if the deficit is greater than 30%.

4. Simulation Results

In order to represent the compliance with the metric defined in (11), a dynamic simulation is considered. The simulation will implement the model in Figure 2 with the parameters in Equations (2)–(5). In order to simulate ERCOT wind power penetration, 18 GW and 25 GW of wind power capacity are considered using the data in [25]. With a time series of wind power output, one can consider persistence as a short term wind power forecast [26,32], so the 5-by-5 min incremental changes in wind power can be assumed as the imbalance to be coped by the SFC system from wind uncertainty (note that ERCOT has a 5-min real time market). For the load component of SFC burden, the short term load forecast error accounts for a mean absolute percentage error of 1.12% (and a 1.39% root mean squared error with 0.00036 variance) [33]. This way, a time series of ERCOT load can be used to construct a time series of short term load forecast error. Then, the AGC gain K_{AGC} is obtained by considering a $\sigma_{NLI_{1m}}$ of 272 MW and 349 MW for the 18 GW and 25 GW of wind penetration, respectively. Additionally, the North American Reliability Corporation (NERC) defines an $\epsilon = 30$ mHz, and a dead-band of 36 mHz. One can use (1) to compute the AGC gains, which are 1.194 MW/Hz and 1.533 MW/Hz for the 18 GW and 25 GW of wind penetration, respectively.

The simulation will consider 1-month long, 4-second step simulations of system frequency for 18 GW and 25GW penetration scenarios. A time series of 1 month of ERCOT load is considered, as well as a 1-month time series of wind power production to obtain the SFC burden time series for the simulated cases. The aim of the simulation is to increase the size of the BESS unit to reach the level of compliance given by (11).

Storage Capacity Results

The simulation considered a BESS with a capacity of 100 MW (P_{nom}) in total. The efficiency of the BESS η is set to 90%. This way, the maximum energy capacity E_{max} is varied to verify dynamic compliance ($E_{min} = 0.1E_{max}$). Then, a base case scenario is simulated to see the behavior of the system, including the BESS with a variable capacity for each wind penetration scenario. The histogram of simulated frequency is shown in Figure 3.

In Figure 3, it was verified that the gain defined in (1) maintains the histogram of the frequency as practically invariant for the scenarios of 18 GW and 25 GW of wind penetration. In order to check the proper functioning of the AGC system, the Control Performance Standard 1 (CPS1) metrics of the North American Electric Reliability Corporation (NERC) was used [34]. The CPS1 metrics statistically evaluates the deviations of minute-to-minute frequency samples over a year from its historical trend. CPS1 compliance was verified with a score of 101.3 and 100.2 for both cases, respectively. CPS1 compliance ensures proper frequency control in terms of system requirements, but do not assure that the BESS has a close tracking of the AGC commands.

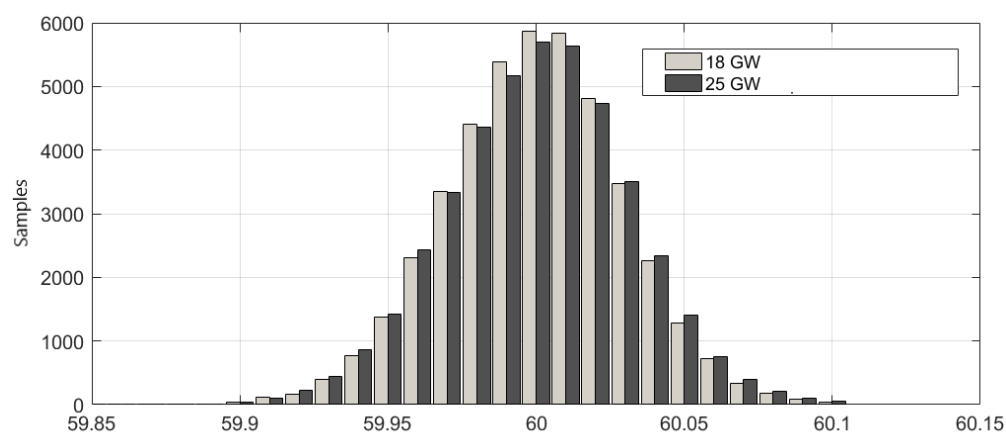


Figure 3. Histograms of system frequency for 18 GW and 25 GW of wind penetration scenarios.

In order to see how close the tracking of the BESS to AGC commands is, this work considers the standard defined in (11). For the simulated case, the BESS deficit is considered for an increasing BESS size. Intuitively, a larger BESS size will allow larger energy movements that will reduce the negative impact of aging-minimizing algorithms. This way, Figure 4 shows the relationship between BESS storage time with the BESS deficit as defined by (11).

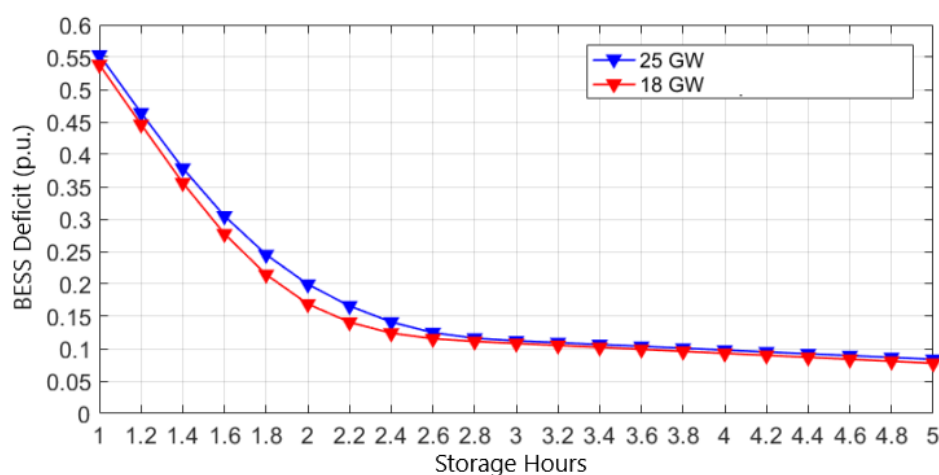


Figure 4. Result of BESS noncompliance for 18 GW and 25 GW of wind penetration scenarios.

In Figure 4, the capacity of the BESS expressed in an hour of storage (maximum storage capacity divided by maximum output power). For 1 h storage, it was found that the BESS was not capable of complying with the standard defined in (11); the minimum capacity for the BESS to comply with the performance criteria was 1.543 h of storage for 18 GW wind penetration and 1.6167 h for 25 GW wind penetration. This is consistent with the larger requirement from the AGC system that the 25 GW scenario represents. Note that, because of the structure of the control framework, the noncompliance of the BESS is compensated for by the action of the rest of the units under the commands of AGC_{GEN} . In other words, this AGC filtered signal frameworks uncover the effects of BESS aging-preventive algorithms on frequency performance, increasing the burden on the rest of the units.

In order to observe the time behavior of the simulated cases, 10-h time responses are considered. Figure 5a shows the BESS power response with respect to the AGC command signal, and Figure 5b the SOC state.

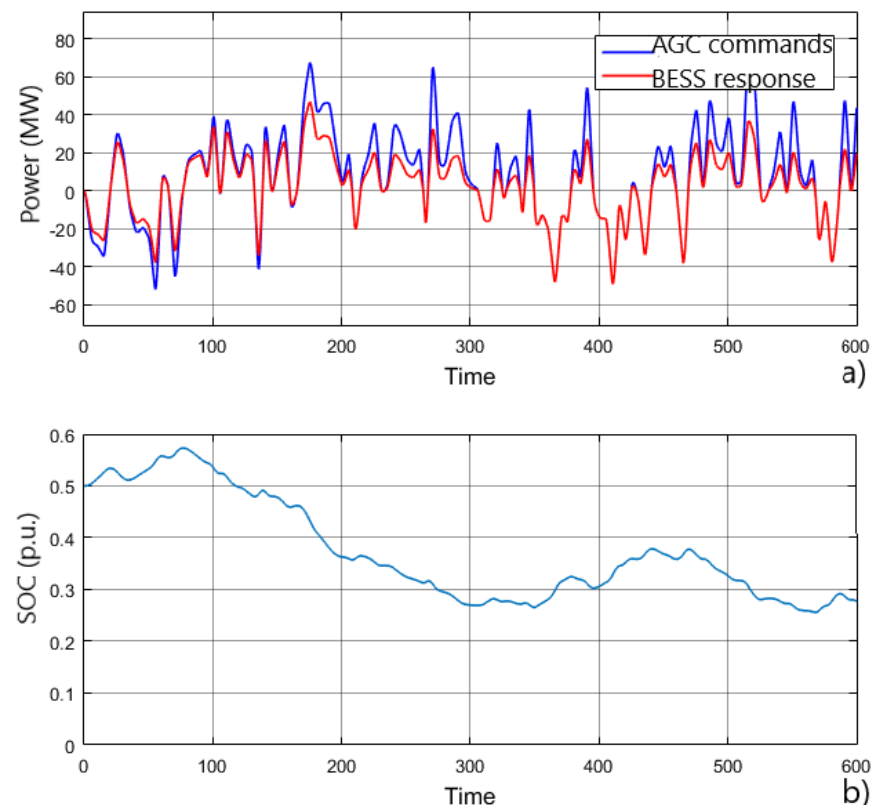


Figure 5. One hundred MW, 1 h BESS power (a) and SoC (b) response for 18 GW of wind power penetration.

It can be seen in Figure 5 that the BESS is prevented from following the AGC command signal by the aging-preventive algorithm. In this case, the upward AGC commands require a power injection from the BESS, which is prevented by the algorithm given the relatively low SoC state. On the contrary, the downward AGC commands are not significantly prevented, since the low SoC allowed the BESS charging.

In order to observe the effect of the aging-preventive algorithm in the entire period under analysis, a 1-month histogram of AGC commands and the BESS response is shown in Figure 6.

In Figure 6, the BESS response is noticeable in failing to track the AGC commands, particularly for high power AGC instructions. This confirms that the phenomenon shown in Figure 6 is not an isolated event but a statistically significant trend. In order to better observe the difference, Figure 7 shows the histogram of the difference between the AGC commands and the BESS power output.

It can be seen in Figure 7 that the aging-preventive algorithm produces a significant difference, accounting for an overall deficit of about 55%.

In contrast, the SoC operation is well-balanced around SoC = 50%, as shown in Figure 8.

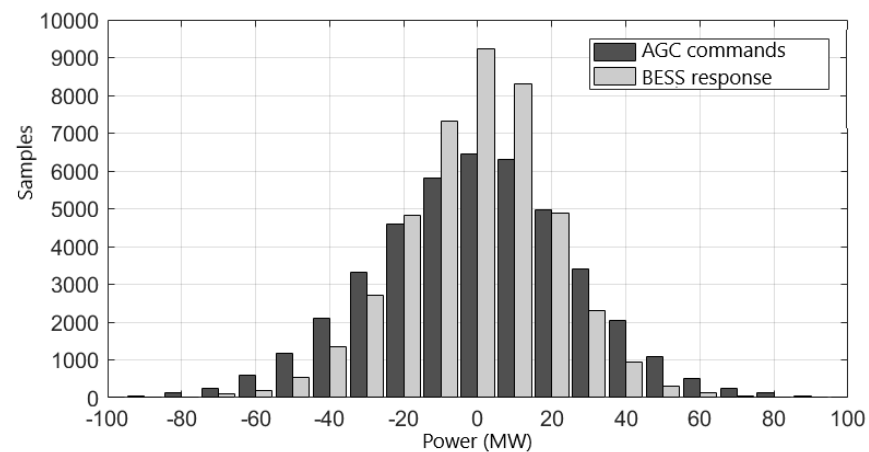


Figure 6. One hundred MW, 1 h BESS response and AGC instructions for 18 GW of wind power scenario.

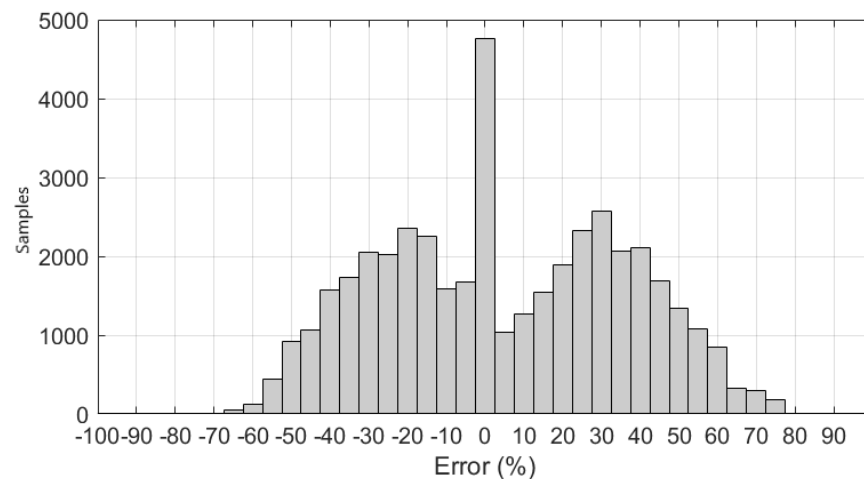


Figure 7. Difference between 100 MW, 1 h BESS power output and the AGC commands for 18 GW of wind power scenario.

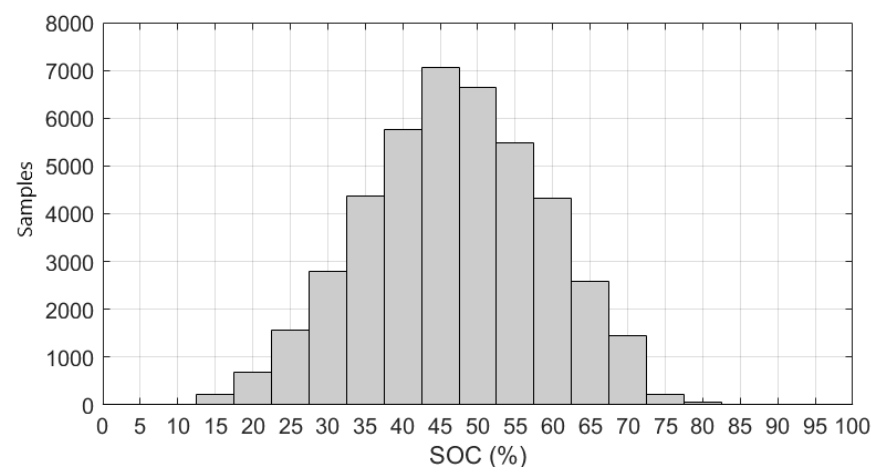


Figure 8. One hundred MW, 1 h BESS SoC for 18 GW of wind power scenario.

The fact that the SoC operation is well-balanced shows that the BESS algorithms are successful in controlling the BESS, regardless of its poor performance to follow the AGC commands as shown in Figure 7. This shows the importance of the BESS size with respect to its performance.

In order to see the impact of the storage time on the performance of the BESS, a similar simulation, but with 3 h of storage, is shown in Figure 9.

The improvement in the response is noticeable as the difference between AGC commands and BESS response in Figure 9 is reduced with respect to Figure 6.

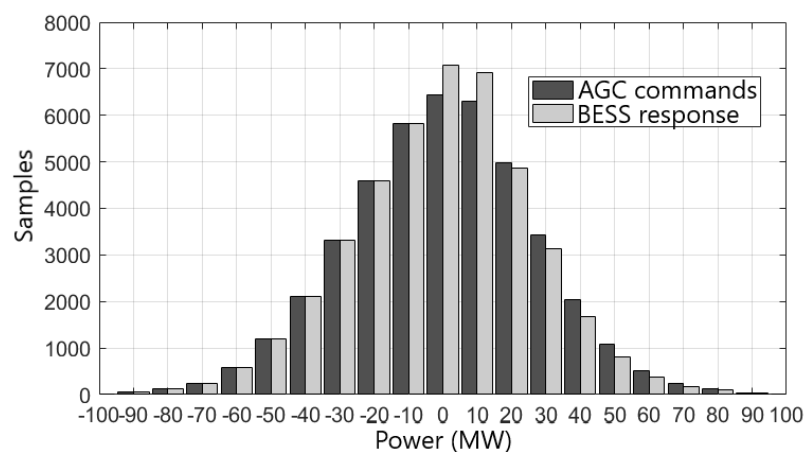


Figure 9. One hundred MW, 3 h BESS response and AGC commands for 18 GW of wind power scenario.

In Figure 10, the histogram of the difference is shown.

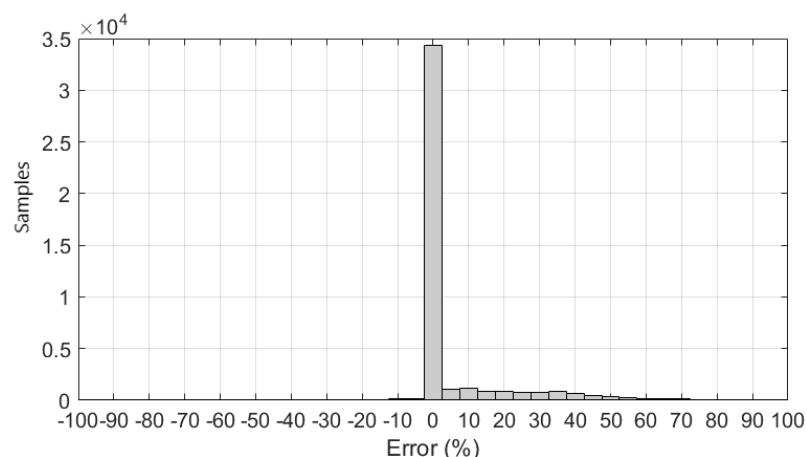


Figure 10. Difference between 100 MW, 3 h BESS power output and AGC commands for 18 GW of wind power scenario.

In contrast to Figure 7, Figure 10 shows that most of the error is around 0%, accounting for an overall deficit of about 8%. This clearly shows the impact of the storage time in the performance of the BESS as an SFC provider.

The SoC histogram for the 3-h BESS case is shown Figure 11.

Similar to the case of 1-h BESS capacity shown Figure 8, the operation of the BESS is well-balanced. This emphasizes the fact that BESS algorithms are mostly concerned about the balance of the BESS to preserve its lifetime and other aspects of the BESS, overlooking the need to maintain a proper tracking of the AGC commands. To summarize, the storage time of a BESS has an important impact on its performance with respect to AGC command tracking.

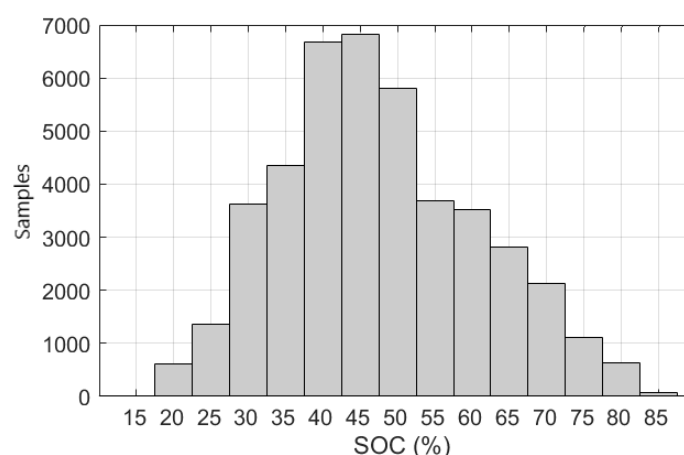


Figure 11. SOC of BESS with 3.1 storage hours for 18 GW scenario of wind power generation in ERCOT.

5. Conclusions and Future Work

The impact of aging-preventing algorithms on BESS AGC performance was investigated. It was found that the size storage time of the BESS had a direct relationship with the compliance of the BESS with the considered performance standard from CAISO. The compliance was also found to be dependent on the penetration level of wind power, and for the two penetration scenarios of 18 GW and 25 GW, the critical storage time was found to be 1.543 and 1.6167 h, respectively. Various simulations were performed, and it was confirmed that BESS storage time is directly related to its performance as an AGC provider. Previous works have overlooked a precise quantification of the BESS capacity in its relationship with the performance standard, and this work has provided such a quantification by means of a long-term dynamic simulation (1 month) using an empirically-validated, reduced-order model of the ERCOT system. This quantification is of significant importance as it uncovers the size of storage systems to maintain AGC performance under wind integration, and makes it possible to understand the costs of maintaining frequency control adequacy with BESS.

As it was verified that storage time affects the compliance of BESS, it is left for future work to perform an economic analysis of the feasibility of the BESS implementation. With the findings of this work, the investment costs of the BESS can be estimated (with a precise value of storage capacity and power), with the certainty of complying with the AGC standard that makes the BESS eligible for reserve payment. To that end, a detailed simulation of the ancillary service market and its sensitivity to wind penetration is necessary to obtain reserve prices and the BESS income. This analysis is left for future work.

Author Contributions: Conceptualization, L.R.-C.; Formal analysis, C.M.; Funding acquisition, H.C.; Investigation, C.M.; Methodology, L.R.-C.; Project administration, H.C.; Software, C.M.; Supervision, H.C.; Validation, A.L. and H.R.C.; Writing—original draft, A.L. and H.C.; Writing—review & editing, H.C., H.R.C. and L.R.-C. All authors have read and agreed to the published version of the manuscript.

Funding: This research was funded by Agencia Nacional de Investigación y Desarrollo: FONDECYT 1191302.

Institutional Review Board Statement: Not applicable.

Informed Consent Statement: Not applicable.

Data Availability Statement: Not applicable.

Conflicts of Interest: The authors declare no conflict of interest.

References

1. Ulbig, A.; Borsche, T.S.; Andersson, G. Impact of low rotational inertia on power system stability and operation. *IFAC Proc. Vol.* **2014**, *19*, 7290–7297. [\[CrossRef\]](#)
2. Mazzeo, D.; Matera, N.; De Luca, P.; Baglivo, C.; Congedo, P.M.; Oliveti, G. A literature review and statistical analysis of photovoltaic-wind hybrid renewable system research by considering the most relevant 550 articles: An upgradable matrix literature database. *J. Clean. Prod.* **2021**, *295*, 126070. [\[CrossRef\]](#)
3. Hannan, M.; Wali, S.; Ker, P.; Rahman, M.A.; Mansor, M.; Ramachandramurthy, V.; Muttaqi, K.; Mahlia, T.; Dong, Z. Battery energy-storage system: A review of technologies, optimization objectives, constraints, approaches, and outstanding issues. *J. Energy Storage* **2021**, *42*, 103023. [\[CrossRef\]](#)
4. Canevese, S.; Gatti, A.; Micolano, E.; Pellegrino, L.; Rapizza, M. Battery Energy Storage Systems for frequency regulation: Simplified aging evaluation. In Proceedings of the 2017 6th International Conference on Clean Electrical Power (ICCEP), Santa Margherita Ligure, Italy, 27–29 June 2017. [\[CrossRef\]](#)
5. Islam, M.M.; Dagli, C.H.; Sun, Z. A Model to Estimate the Lifetime of BESS for the Prosumer Community of Manufacturers with OGS. *Procedia Comput. Sci.* **2020**, *168*, 186–194. [\[CrossRef\]](#)
6. Xu, D.; Kuo, X.; Nan, L.; Yaping, H.; Zhe, Z.; Qixing, L. Optimal Design and Application of AGC Performance Index Measurement Standards for Generating Units Adapted To the China Southern Regional Frequency Regulation Auxiliary Service Market. *J. Phys. Conf. Ser.* **2021**, *1802*, 032138. [\[CrossRef\]](#)
7. Sadeghi-Mobarakeh, A.; Mohsenian-Rad, H. Performance Accuracy Scores in CAISO and MISO Regulation Markets: A Comparison Based on Real Data and Mathematical Analysis. *IEEE Trans. Power Syst.* **2018**, *33*, 3196–3198. [\[CrossRef\]](#)
8. Nguyen, T.A.; Byrne, R.H.; Concepcion, R.J.; Gyuk, I. Maximizing revenue from electrical energy storage in MISO energy & frequency regulation markets. *IEEE Power Energy Soc. Gen. Meet.* **2018**, *2018*, 1–5. [\[CrossRef\]](#)
9. Yang, Y.; Bremner, S.; Menictas, C.; Kay, M. Battery energy storage system size determination in renewable energy systems: A review. *Renew. Sustain. Energy Rev.* **2018**, *91*, 109–125. [\[CrossRef\]](#)
10. Mulleriyawage, U.; Shen, W. Impact of demand side management on optimal sizing of residential battery energy storage system. *Renew. Energy* **2021**, *172*, 1250–1266. [\[CrossRef\]](#)
11. Sanjareh, M.B.; Nazari, M.H.; Gharehpetian, G.B.; Ahmadihangar, R.; Rosin, A. Optimal scheduling of HVACs in islanded residential microgrids to reduce BESS size considering effect of discharge duration on voltage and capacity of battery cells. *Sustain. Energy Grids Netw.* **2021**, *25*, 100424. [\[CrossRef\]](#)
12. Uchman, W.; Kotowicz, J.; Li, K.F. Evaluation of a micro-cogeneration unit with integrated electrical energy storage for residential application. *Appl. Energy* **2021**, *282*, 116196. [\[CrossRef\]](#)
13. Anselma, P.G.; Kollmeyer, P.; Lempert, J.; Zhao, Z.; Belingardi, G.; Emadi, A. Battery state-of-health sensitive energy management of hybrid electric vehicles: Lifetime prediction and ageing experimental validation. *Appl. Energy* **2021**, *285*, 116440. [\[CrossRef\]](#)
14. Li, S.; He, H.; Su, C.; Zhao, P. Data driven battery modeling and management method with aging phenomenon considered. *Appl. Energy* **2020**, *275*, 115340. [\[CrossRef\]](#)
15. Li, Y.; Sheng, H.; Cheng, Y.; Stroe, D.I.; Teodorescu, R. State-of-health estimation of lithium-ion batteries based on semi-supervised transfer component analysis. *Appl. Energy* **2020**, *277*, 115504. [\[CrossRef\]](#)
16. Li, X.; Huang, Z.; Tian, J.; Tian, Y. State-of-charge estimation tolerant of battery aging based on a physics-based model and an adaptive cubature Kalman filter. *Energy* **2021**, *220*, 119767. [\[CrossRef\]](#)
17. Šeruga, D.; Gosar, A.; Sweeney, C.A.; Jaguemont, J.; Van Mierlo, J.; Nagode, M. Continuous modelling of cyclic ageing for lithium-ion batteries. *Energy* **2021**, *215*, 119079. [\[CrossRef\]](#)
18. Li, J.; Wang, D.; Deng, L.; Cui, Z.; Lyu, C.; Wang, L.; Pecht, M. Aging modes analysis and physical parameter identification based on a simplified electrochemical model for lithium-ion batteries. *J. Energy Storage* **2020**, *31*, 101538. [\[CrossRef\]](#)
19. Calero, F.; Cañizares, C.A.; Bhattacharya, K. Dynamic Modeling of Battery Energy Storage and Applications in Transmission Systems. *IEEE Trans. Smart Grid* **2021**, *12*, 589–598. [\[CrossRef\]](#)
20. Rancilio, G.; Rossi, A.; Di Profio, C.; Alborghetti, M.; Galliani, A.; Merlo, M. Grid-Scale BESS for Ancillary Services Provision: SoC Restoration Strategies. *Appl. Sci.* **2020**, *10*, 4121. [\[CrossRef\]](#)
21. Cheng, Y.; Tabrizi, M.; Sahni, M.; Povedano, A.; Nichols, D. Dynamic Available AGC Based Approach for Enhancing Utility Scale Energy Storage Performance. *IEEE Trans. Smart Grid* **2014**, *5*, 1070–1078. [\[CrossRef\]](#)
22. Doenges, K.; Egido, I.; Sigrist, L.; Lobato Miguélez, E.; Rouco, L. Improving AGC Performance in Power Systems with Regulation Response Accuracy Margins Using Battery Energy Storage System (BESS). *IEEE Trans. Power Syst.* **2020**, *35*, 2816–2825. [\[CrossRef\]](#)
23. Perez, A.; Moreno, R.; Moreira, R.; Orchard, M.; Strbac, G. Effect of Battery Degradation on Multi-Service Portfolios of Energy Storage. *IEEE Trans. Sustain. Energy* **2016**, *7*, 1718–1729. [\[CrossRef\]](#)
24. Chavez, H.; Baldick, R.; Matevosyan, J. CPS1 compliance-constrained AGC gain determination for a single-balancing authority. *IEEE Trans. Power Syst.* **2014**, *29*, 1481–1488. [\[CrossRef\]](#)
25. Chávez, H.; Lee, D.; Baldick, R. CPS1-Compliant Regulation Using a PSD Analysis of Wind Expansion in a Single Balancing Authority. *IEEE Trans. Power Syst.* **2015**, *6*, 976–983. [\[CrossRef\]](#)
26. Chavez, H.; Baldick, R.; Sharma, S. Regulation adequacy analysis under high wind penetration scenarios in ERCOT Nodal. *IEEE Trans. Sustain. Energy* **2012**, *3*, 743–750. [\[CrossRef\]](#)

-
27. Lee, D.; Kim, J.; Baldick, R. Stochastic optimal control of the storage system to limit ramp rates of wind power output. *IEEE Trans. Smart Grid* **2013**, *4*, 2256–2265. [[CrossRef](#)]
 28. Atalay, S.; Sheikh, M.; Mariani, A.; Merla, Y.; Bower, E.; Widanage, W.D. Theory of battery ageing in a lithium-ion battery: Capacity fade, nonlinear ageing and lifetime prediction. *J. Power Source* **2020**, *478*, 229026. [[CrossRef](#)]
 29. Alabi, T.M.; Lu, L.; Yang, Z. A novel multi-objective stochastic risk co-optimization model of a zero-carbon multi-energy system (ZCMES) incorporating energy storage aging model and integrated demand response. *Energy* **2021**, *226*, 120258. [[CrossRef](#)]
 30. Rancilio, G.; Lucas, A.; Kotsakis, E.; Fulli, G.; Merlo, M.; Delfanti, M.; Masera, M. Modeling a Large-Scale Battery Energy Storage System for Power Grid Application Analysis. *Energies* **2019**, *12*, 3312. [[CrossRef](#)]
 31. Zhang, S.; Liu, H.; Wang, F.; Yan, T.; Wang, K. Secondary frequency control strategy for BESS considering their degree of participation. *Energy Rep.* **2020**, *6*, 594–602. [[CrossRef](#)]
 32. Jaseena, K.; Kovoov, B.C. Deterministic weather forecasting models based on intelligent predictors: A survey. *J. King Saud Univ. Comput. Inf. Sci.* **2020**. [[CrossRef](#)]
 33. Mamun, A.A.; Sohel, M.; Mohammad, N.; Haque Sunny, M.S.; Dipta, D.R.; Hossain, E. A Comprehensive Review of the Load Forecasting Techniques Using Single and Hybrid Predictive Models. *IEEE Access* **2020**, *8*, 134911–134939. [[CrossRef](#)]
 34. Jaleeli, N.; VanSlyck, L. NERC's new control performance standards. *IEEE Trans. Power Syst.* **1999**, *14*, 1092–1099. [[CrossRef](#)]